

The Inclination, Pitch Angle and Forbidden Radius of Spiral Arms of PGC 35105 *

Tao Hu¹, Zheng-Yi Shao^{2,3} and Qiu-He Peng^{1,4,5}

¹ Department of Astronomy, Nanjing University, Nanjing 210093; taohu@nju.edu.cn

² Shanghai Astronomical Observatory, Chinese Academy of Sciences, Shanghai 200030

³ Joint Institute for Galaxies and Cosmology, Chinese Academy of Sciences, Shanghai, 200030

⁴ Joint Astrophysics Center of Chinese Academy of Sciences-Peking University, Beijing 100871

⁵ The Open Laboratory of Cosmic Ray and High Energy Astrophysics, Chinese Academy of Sciences, Beijing 100049

Received 2005 June 10; accepted 2005 August 22

Abstract We have studied some properties including surface brightness in the u , g , r , i , and z bands of the nearly face-on galaxy PGC 35105. By subtracting a model surface brightness distribution from the observed image we obtain the residual image that shows only the spiral arms freed from the contamination by the bulge. From this we measured the inclination, pitch angle, and forbidden radius (identified with the innermost point of the arm) for each of the two arms; and that for each of the five observing bands. We found these three parameters are largely independent of the observing band.

Key words: galaxies: fundamental parameters — galaxies: spiral — galaxies: structure — galaxies: surface brightness — galaxies: individual (PGC 35105)

1 INTRODUCTION

A spiral galaxy consists of a halo, a bulge and a disk. It would show spiral structure when it is face-on. Freeman (1970) investigated the surface brightness of disk galaxies and showed that the surface brightness — radius plot for a disk of spiral galaxy could be described by an exponential decrease law, i.e.,

$$I_d(r) = I_{0d} \exp(-r/r_d), \quad (1)$$

where I_{0d} is the central surface brightness of the disk, r the radius and r_d the scale length of the disk.

In the plot of $\lg I$ versus r , the outermost points of spiral galaxies tend to lie on straight lines, that is, at large radii the surface brightness obeys Equation (1). It is the surface brightness distribution to fit the outer brightness profile of disk galaxies.

In fact, we can observe that, in many profiles of disk galaxies, it is significantly brighter near the center than the exponential law in the outer part. In 1959, de Vaucouleurs opted for a radial luminosity distribution of spiral galaxies that can accurately be described by a combination of a bulge and an exponential disk. The images of disk galaxies show that in most cases the additional

* Supported by the National Natural Science Foundation of China.

brightness is contributed by a bulge, which could well obey the $r^{1/4}$ decrease law (de Vaucouleurs 1948),

$$I_b(r) = I_{0b} \exp[-(r/r_b)^{1/4}], \quad (2)$$

where I_{0b} is the central surface brightness, r is the radial distance, and r_b the scale length of bulge. Some useful references are Simien & de Vaucouleurs (1986), de Jong & van de Kruit (1994), Walterbos & Kennicutt (1987), and Wevers, Van der Kruit & Allen (1986). It turns out that a fit to the composite profile of disk galaxy can be of the form of a bulge-disk decomposition.

Equations (1) and (2) can be represented by other forms, i.e., the disk composition

$$I_d(r) = I_{ed} \exp[-1.68(r/r_{ed} - 1)], \quad (3)$$

and the bulge composition

$$I_b(r) = I_{eb} \exp\{-7.67[(r/r_{eb})^{1/4} - 1]\}, \quad (4)$$

where r_{ed} is the effective radius (radius that encloses half the total light of the disk), and I_{ed} is the surface brightness at this radius, r_{eb} and I_{eb} are the corresponding parameters for the bulge.

In practice, the surface brightness I is in units of mag arcsec^{-2} , the radius r in arcsec, and a plot of $\lg I$ versus radius r defines the surface-brightness profile, $\lg I$ can be derived from Eqs. (3) and (4). Then we obtain the expression (disk composition)

$$m_d = m_{ed} + (2.5/\ln 10) \times 1.68(r/r_{ed} - 1), \quad (5)$$

and the expression (bulge composition)

$$m_b = m_{eb} + (2.5/\ln 10) \times 7.67[(r/r_{eb})^{1/4} - 1], \quad (6)$$

where, m_d and m_b are the decomposed surface brightnesses in magnitudes, m_{ed} is the magnitude at radius r_{ed} , and m_{eb} at r_{eb} .

After fitting the observed surface brightness profile with a sum of Eqs. (5) and (6), we obtain the parameters (m_{ed} , r_{ed} , m_{eb} and r_{eb}). Then we obtain the combined magnitude m at radius r .

The structure of this paper is as follows. The forbidden radius around the center of galaxy is described in Section 2. The inclination of galactic disk is discussed in Section 3. In Section 4 we determine the pitch angle of a spiral arm and give an expression for the error. Our results are presented in Section 5, and a discussion and conclusions are given in Section 6.

2 FORBIDDEN RADIUS AROUND THE CENTER OF A SPIRAL GALAXY

It may be noted that a spiral arm does not extend into a forbidden region (radius r_0) around the galactic center. The forbidden radius r_0 can be obtained by measuring the most inward point of the spiral arm in the image. Column 1 of Figure 1 displays the observed images of the spiral galaxy PG35105 in the u , g , r , i , and z bands. The spiral arms are easily seen in these images in general. However, in the central region, the spiral arms are occasionally blurred by the bulge component. So, we could only give approximate estimates of the innermost points of the arms, under personal preconceptions on the pattern of the arms: it is not an easy matter to determine the exact value of the forbidden radius r_0 under these circumstances.

In view of this, we first find the best fitting combination of Eqs. (5) and (6) to the observed image. Then, the fit is subtracted from the observed image, giving a residual image that shows only the spiral arms without contamination by the bulge. We can then measure the innermost point of the spiral arm free of blurring and without personal prejudice, and so determine the exact forbidden radius.

Then, we can also further investigate the mathematical form of the spiral structure, and acquire the inclination and the pitch angle by directly fitting the shape of the spiral arm in the residual image.

However, in fact, there are two main errors in this approach, one is the error in the best-fitting to the surface brightness profile, the other is the seeing. Examining the sum of the pixel flux (pixel value) in the residual can reveal if the model is proper or not. When the fit is good, the total flux in the residual image will be small compared to that of the original image.

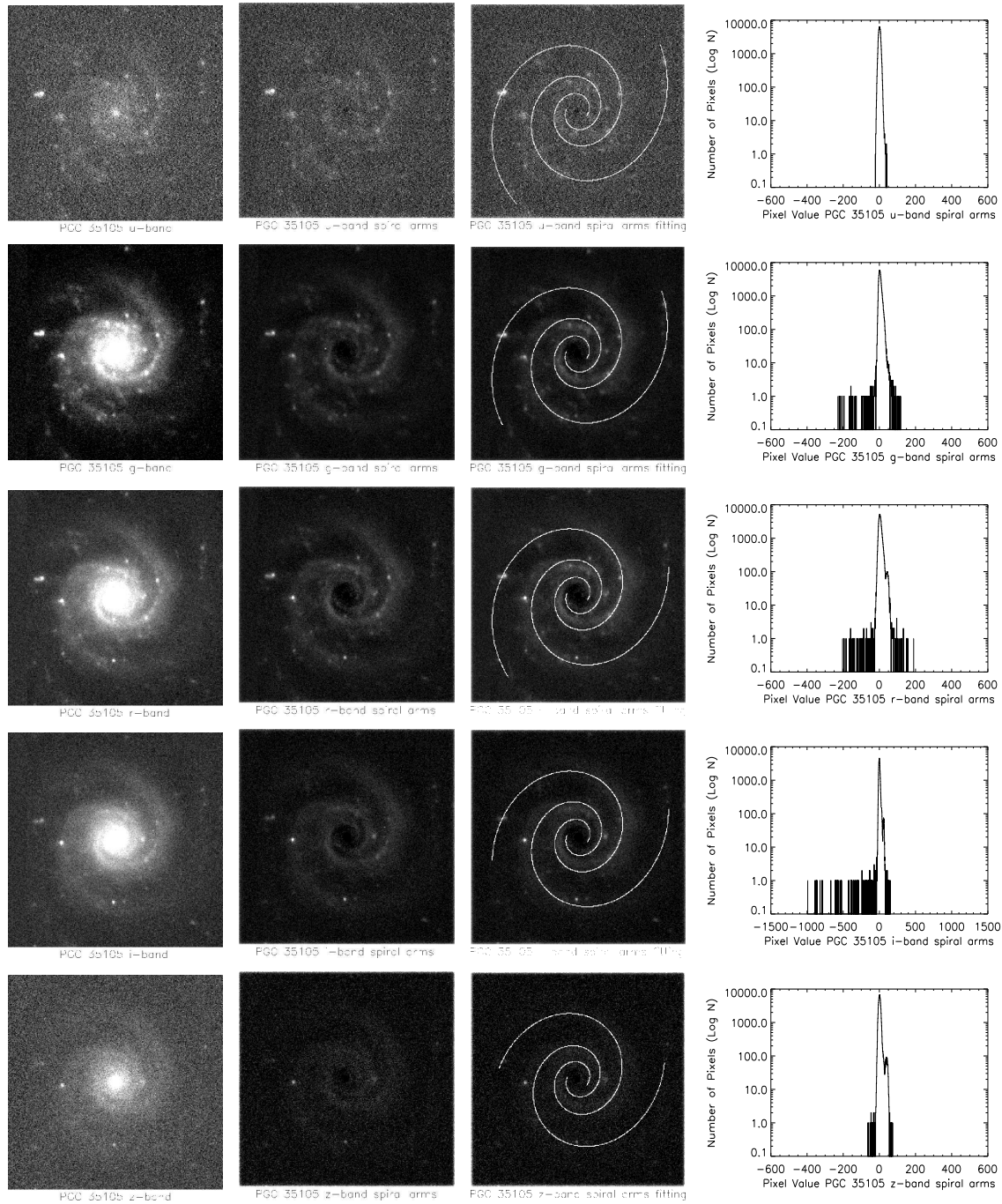


Fig. 1 From left to right, Column 1: observed image of the spiral galaxy PGC 35105; Column 2: residual image after the decomposition model fit has been subtracted from the observed image; Column 3: fitting of the spiral structure; Column 4: histogram showing the number of pixels, N (on a logarithmic scale) with a given flux (reckoned from a mean value). The rows from top down refer to the five observing bands.

3 INCLINATION OF THE GALACTIC DISK

Inclination of the galactic disk is the angle between the galactic plane and the tangent plane of the celestial sphere. If we assume that the thickness of the galactic disk is infinite thin, the inclination (γ) is given by

$$\gamma = \arccos\left(\frac{d}{D}\right), \quad (7)$$

where D and d are the major and minor isophotal axes of the disk, respectively. In fact, due to the finite thickness disk and the bulge, the error of the inclination obtained by Equation (7) is not negligible. Aaronson et al. (1980) refined the expression to

$$\gamma = \arccos\sqrt{1.042\left(\frac{d}{D}\right)^2 - 0.042 + 0.052}^1. \quad (8)$$

It may be noted that the value given by Equation (8) is still not exact enough. The reason is that the values of d and D are only approximations due to errors. Ma et al. (1997, 1998) proposed a method of determining the inclination of a spiral galaxy by fitting a spiral arm with a logarithmic spiral. We can obtain a first approximate value (γ_0) from Eq. (8), then we adjust the value of γ around γ_0 , until the logarithmic spiral curve fits the spiral arm in the residual image. D_{25} and d_{25} in Eq. (8) denote respectively the measured apparent major and minor isophotal diameters defined by surface brightness level $\mu = 25.0B$ mag per square arcsecond according to RC3 (Third Reference Catalogue of Bright Galaxies).

4 DETERMINATION OF PITCH ANGLE

Hu et al. (2006) explained the method to obtain the pitch angle of the spiral arm, together with a formula for the error. They determine the pitch angle by fitting a spiral to the arm in the galaxy image of the form (ρ and θ being the polar coordinates),

$$\rho(\theta, \gamma) = \rho_0 \frac{f(\theta_0, \gamma)}{f(\theta, \gamma)} \exp\left[\frac{m}{\Lambda} \cdot B(\theta, \gamma)\right], \quad (9)$$

where

$$f(\theta, \gamma) = \sqrt{\sin^2 \theta + \cos^2 \theta \cdot \cos^2 \gamma}, \quad (10)$$

and

$$B(\theta, \gamma) = \arctan \frac{\tan \theta}{\cos \gamma} - \arctan \frac{\tan \theta_0}{\cos \gamma} \pm k\pi, \quad (11)$$

with k an integer.

Let (ρ_i, θ_i) be the coordinates of the points on the spiral arm, we can derive Λ according to the least squares principle, i.e., by minimizing the quantity

$$\sum_{i=1}^n [\rho_i - \rho(\theta_i, \gamma)]^2 = \min. \quad (12)$$

5 SAMPLE AND RESULTS

For our sample, we selected from RC3 the galaxy PGC 35105 because it is nearly face-on, its minor to major axis ratio being larger than 0.8. The images are taken from SDSS DR3.

The parameters of the bulge-disk decomposition were obtained by fitting the observed surface brightness profile with a sum of Eqs. (5) and (6). In Table 1, Columns 3, 4, 5, and 6 list, respectively, the parameters m_{ed} , r_{ed} , m_{eb} , and r_{eb} of PGC 35105 in the u , g , r , i , and z bands. In the i -band,

¹ This is essentially the same equation as Eq. (30) in the author's previous paper (ChJAA 2006, 6(1), p.50), except that, there, the last value was *wrongly* printed as '0.52'; the correct value is the value given here, 0.052.

Table 1 Bulge and Disk Parameters of PGC 35105 in Five Bands

PGC	Band	m_{eb} [mag arcsec $^{-2}$]	r_{eb} [arcsec]	m_{ed} [mag arcsec $^{-2}$]	r_{ed} [arcsec]
(1)	(2)	(3)	(4)	(5)	(6)
35105	<i>u</i>	26.63 \pm 0.05	14.53 \pm 0.38	25.02 \pm 0.04	19.67 \pm 0.28
	<i>g</i>	25.30 \pm 0.04	16.97 \pm 1.01	23.54 \pm 0.03	20.10 \pm 0.61
	<i>r</i>	24.55 \pm 0.04	15.94 \pm 0.33	22.85 \pm 0.03	18.06 \pm 0.35
	<i>i</i>	23.38 \pm 0.04	6.51 \pm 0.19	22.27 \pm 0.02	16.65 \pm 0.21
	<i>z</i>	23.82 \pm 0.04	14.02 \pm 0.31	22.24 \pm 0.03	15.23 \pm 0.31

Table 2 Parameters of PGC 35105 in *u*, *g*, *r*, *i* and *z* Bands

PGC	Band	γ [$^{\circ}$]	r_0 [kpc]	$\Lambda \pm d\Lambda/\Lambda$ [%]	μ [$^{\circ}$]	$\Delta F_r/F_m$ [%]	$\bar{\gamma}$ [$^{\circ}$]	$\bar{\mu}$ [$^{\circ}$]	\bar{r}_0 [kpc]
(1)	(2)	(3)	(4)	(5)	(6)	(7)	(8)	(9)	(10)
35105 a-spiral arm	<i>u</i>	27.06	1.772	9.72 \pm 36.5	11.63	2.2	26.69	11.67	1.788
	<i>g</i>	26.36	1.809	9.64 \pm 21.7	11.72	8.4			
	<i>r</i>	26.90	1.803	9.68 \pm 27.6	11.67	5.1			
	<i>i</i>	26.23	1.797	9.67 \pm 30.1	11.69	3.8			
	<i>z</i>	26.89	1.757	9.69 \pm 29.9	11.66	2.2			
35105 b-spiral arm	<i>u</i>	27.90	1.801	9.23 \pm 31.2	12.23	2.2	26.77	12.15	1.833
	<i>g</i>	26.51	1.925	9.38 \pm 26.9	12.04	8.4			
	<i>r</i>	26.22	1.810	9.33 \pm 23.4	12.10	5.1			
	<i>i</i>	26.46	1.822	9.23 \pm 25.8	12.23	3.8			
	<i>z</i>	26.78	1.805	9.28 \pm 26.7	12.16	2.2			

$r_{\text{eb}} = 6.51''$, which is much smaller than the r_{eb} values for the *u*, *g*, *r*, and *z* bands, the reason is due to the ill-PSF in the *i*-band (Wu et al. 2005).

Images referring to the five observing bands are displayed in the successive rows of Figure 1. In this figure, Column 1 is the observed image, with the left spiral arm labelled “a”, and the right one, labelled “b”. Column 2 is the residual image, obtained after subtracting the “decomposition model” fit from the observed image. Column 3 shows the fitting of the pattern of spiral structure. Column 4 gives the histogram of the number of pixels, N (on a logarithmic scale) with a given flux (reckoned from the mean value) in the residual image. From this histogram and the flux zero we can calculate the total flux in the residual image (the value ΔF_r refers to the flux ratio of Table 2, Column 7).

Tables 2 lists the results for the two arms (a) and (b) in the five passbands. Specifically, Column 3 gives the inclination; Column 4, the forbidden radius; Column 5, the winding parameter and its error; and Column 6, the pitch angle. Column 7 gives the flux ratio of spiral to system, $\Delta F_r/F_m$, ΔF_r being the sum over the residual flux histogram shown in Figure 1 Column 4, and F_m is the sum over the original image (Fig. 1, Column 1). The mean inclination, pitch angle, and forbidden radius are given in Columns 8, 9 and 10, respectively.

6 DISCUSSION AND CONCLUSIONS

1. In Table 2, Column 5 shows that all five bands yield approximately the same forbidden radius for either one of the two arms, and the differences being less than 4%. It implies that the forbidden radius is, to a good approximation, independent of the observing band.
2. We also found that the different observing bands gave about the same pitch angle of the spiral arm leading to the conclusion that the pitch angle is a constant for a given spiral arm, with no dependence on the observing band. In Table 2, Column 3 shows that the inclination γ is also a constant.

3. As listed in Table 2, the pitch angles of the two spiral arms a and b, are, respectively, 11.67° and 12.15° , with a difference of less than 4.2%. Their forbidden radii are 1.788 and 1.833 kpc, with a difference of 2.5%.
4. In Table 2, Column 7 shows that the flux ratio of spiral-to-system we found is less than 8.4%. This is reasonable since the total residual flux from a good fit should be small compared to the total flux in the original image.
5. The image in the u band is not so clear. The main contributor to light in this band is the young population, but a larger fraction of the light is obscured by the dust component. At the much redder z band, the influence of dust becomes much smaller and the older population will show up more clearly.

Acknowledgements We would like to thank the referee for the careful reviews of this paper. This research is supported by the National Natural Science Foundation of China (Nos. 10573011, 10273006, 10273016 and 10333060), and the Doctoral Program Foundation of State Education Commission of China.

References

- Aaronson M., Mould J., Huchra J., 1980, *ApJ*, 237, 655
de Vaucouleurs G., 1948, *Ann. Astrophys.*, 11, 247
de Vaucouleurs G., 1959, *AJ*, 64, 397
de Vaucouleurs G., de Vaucouleurs A., Corwin H. G. Jr, et al., 1991, *Third Reference Catalogue of Bright Galaxies*, New York: Springer
de Jong R. S., van der Kruit P. C., 1994, *A&AS*, 106, 451
Freeman K. C., 1970, *ApJ*, 160, 811
Hu T., Peng Q. H., Zhao Y. H., 2006, *ChJAA*, 6(1), 43
Ma J., Peng Q. H., Gu Q. S., 1997, *ApJ*, 400, L41
Ma J., Peng Q. H., Gu Q. S., 1998, *A&AS*, 130, 449
Simien F., de Vaucouleurs G., 1986, *ApJ*, 302, 564
Walterbos R. A. M., Kennicutt R. C., 1987, *A&AS*, 69, 311
Wevers B. M. H. R., van der Kruit P. C., Allen R. J., 1986, *A&AS*, 66, 505
Wu H., Shao Z. Y., Mo H. J., et al., 2006, *ApJ*, 622, 244